WDR72 Mutations Associated with Amelogenesis Imperfecta and Acidosis

H. Zhang[1], M. Koruyucu[2], F. Seymen[2], Y. Kasimoglu[2], J.-W. Kim[3,4] (iD),
S. Tinawi[1], C. Zhang[1], M.L. Jacquemont[5], A.R. Vieira[6,7] (iD), J.P. Simmer[1],
and J.C.C. Hu[1]

Abstract

Dental enamel malformations, or amelogenesis imperfecta (AI), can be isolated or syndromic. To improve the prospects of making a successful diagnosis by genetic testing, it is important that the full range of genes and mutations that cause AI be determined. Defects in WDR72 (WD repeat-containing protein 72; OMIM *613214) cause AI, type IIA3 (OMIM #613211), which follows an autosomal recessive pattern of inheritance. The defective enamel is normal in thickness, severely hypomineralized, orange-brown stained, and susceptible to attrition. We identified 6 families with biallelic WDR72 mutations by whole exome sequence analyses that perfectly segregated with the enamel phenotype. The novel mutations included 3 stop-gains [NM_182758.2: c.377G>A/p.(Trp126*), c.1801C>T/p.(Arg601*), c.2350A>T/p.(Arg784*)], a missense mutation [c.1265G>T/p.(Gly422Val)], and a 62,138–base pair deletion (NG_017034.2: g.35441_97578del62138) that removed WDR72 coding exons 3 through 13. A previously reported WDR72 frameshift was also observed [c.1467_1468delAT/p.(Val491Aspfs*8)]. Three of the affected patients showed decreased serum pH, consistent with a diagnosis of renal tubular acidosis. Percentiles of stature and body weight varied among 8 affected individuals but did not show a consistent trend. These studies support that WDR72 mutations cause a syndromic form of AI and improve our ability to diagnose AI caused by WDR72 defects.

Keywords: hypomaturation, enamel, tooth, kidney, distal renal tubule, SLC24A4

Introduction

The process of dental enamel formation, or amelogenesis, depends on the contributions of many genes. About 90 inherited conditions, mostly syndromes, include enamel malformations as a phenotype (Wright et al. 2015). About 20 genes contribute to the etiology of nonsyndromic (isolated) forms of amelogenesis imperfecta (AI; Smith et al. 2017). Because primary teeth begin to erupt in the first year and are all erupted by 3 y of age (Burgueno Torres et al. 2015), there is an early presentation of dental enamel malformations to clinicians. In many syndromes, the enamel phenotype precedes systemic manifestations and is the only apparent sign at the time of initial diagnosis. Abnormally thin (hypoplastic) enamel is characteristic of an early disturbance during amelogenesis, and soft enamel of normal thickness (hypomaturation) is characteristic of a late disturbance; however, oral and radiographic examination of the enamel presentation cannot discriminate between isolated and syndromic forms of AI. Despite this, patients with syndromic AI with an early diagnosis that specifically defines the cause and nature of their inherited condition may greatly benefit from interventions to improve their prognosis. It is therefore incumbent on dentists who identify inherited enamel malformations of unknown cause to refer their patients for a genetic consultation. This report is part of an ongoing research effort to identify the genes and mutations that cause inherited enamel malformations so that routine genetic tests can identify the genetic etiology of a patient's condition.

The discovery that WDR72 (WD repeat-containing protein 72; OMIM *613214) causes autosomal recessive hypomaturation AI was the first evidence that WDR72 is necessary for dental enamel formation (El-Sayed et al. 2009). Mouse studies determined that WDR72 is an intracellular protein that is

[1]Department of Biologic and Materials Sciences, School of Dentistry, University of Michigan, Ann Arbor, MI, USA
[2]Department of Pedodontics, Faculty of Dentistry, Istanbul University, Istanbul, Turkey
[3]Department of Molecular Genetics and Dental Research Institute, School of Dentistry, Seoul National University, Seoul, Republic of Korea
[4]Department of Pediatric Dentistry and Dental Research Institute, School of Dentistry, Seoul National University, Seoul, Republic of Korea
[5]Génétique Médicale, Pôle femme-mère-enfant, CHU la Réunion site GHSR, BP 350-97448 Saint Pierre Cedex
[6]Departments of Oral Biology and Pediatric Dentistry, Center for Craniofacial and Dental Genetics, School of Dental Medicine, University of Pittsburgh, Pittsburgh, PA, USA
[7]Department of Human Genetics, Graduate School of Public Health; Clinical and Translational Science Institute, University of Pittsburgh, Pittsburgh, PA, USA

A supplemental appendix to this article is available online.

Corresponding Author:
J.-W. Kim, Department of Molecular Genetics, Department of Pediatric Dentistry and Dental Research Institute, School of Dentistry, Seoul National University, 101 Daehak-ro, Jongno-gu, Seoul, 03080, Korea.
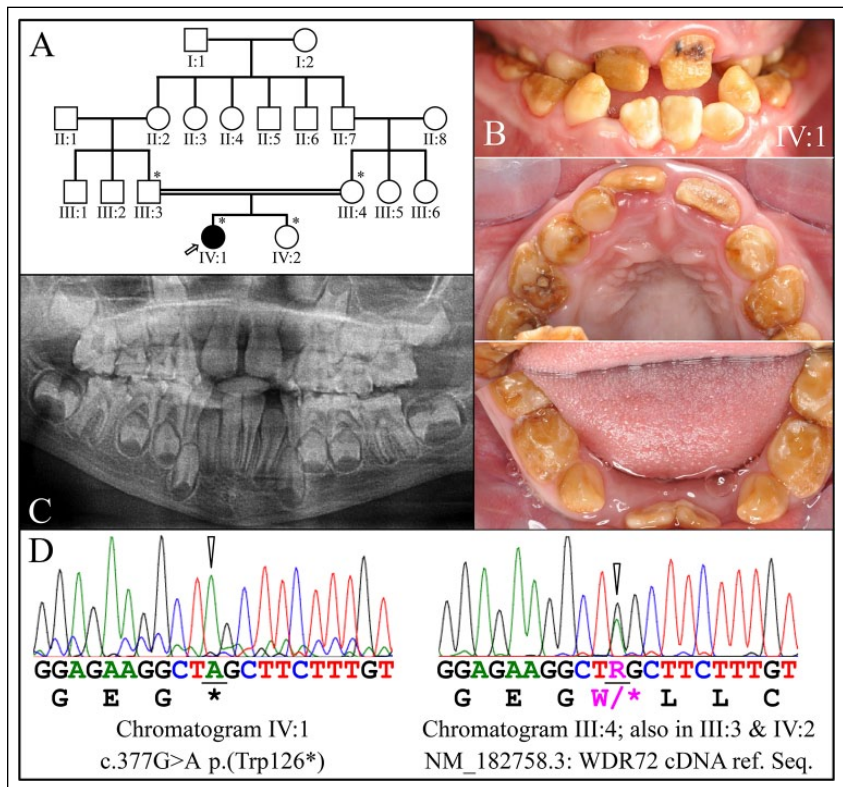Email: pedoman@snu.ac.kr

Figure 1. Family 1. (**A**) Pedigree of family 1. The proband (IV:1) is the only affected member and is indicated by an arrow. The asterisks (*) indicate the 4 family members recruited for this study. The double line connecting the father (III:3) and the mother (III:4) of the proband indicates consanguinity. (**B**) Clinical photos of the proband's dentition in the mixed dentition stage (age, 8 y). Hypomaturation amelogenesis imperfecta is evident in the primary and secondary dentitions, which were stained brown and had undergone rapid attrition. Black stains on the maxillary permanent central incisors suggested the early onset of dental caries. (**C**) Panoramic radiograph of the proband. The enamel layer was barely visible radiographically, although the sizes and shapes of the crowns were within normal limits at the time of eruption, suggesting that enamel layer thickness was within normal limits. (**D**) DNA sequence chromatograms confirmed that the proband was homozygous for the *WDR72* c.377G>A mutation that introduced a p.(Trp126*) stop gain in exon 5 (left). The mother (III:3), father (III:4), and sister (IV:2) of the proband were all heterozygous for this defect (right).

upregulated in maturation-stage ameloblasts (El-Sayed et al. 2009; Lee et al. 2010; Katsura et al. 2014; Simmer et al. 2014). Two *Wdr72* knockout mice were generated and characterized, revealing profound maturation-stage enamel deficits (Katsura et al. 2014; Wang et al. 2015). The *Wdr72*-null enamel exhibited normal thickness and rod/interrod architecture. However, enamel proteins were retained in the extracellular matrix; the final enamel layer was only 10% as hard as normal; and SLC24A4, the key transporter of calcium into maturing enamel, failed to localize along the distal ameloblast membrane (Wang et al. 2015). By analogy to its WD40 protein homologues, WDR72 is a scaffolding protein without intrinsic enzymatic activity that forms multiple beta propeller blade structures, which serve as docking platforms for the assembly of protein complexes (Stirnimann et al. 2010; Xu and Min 2011).

Proximal renal tubular acidosis has long been associated with enamel defects (Winsnes et al. 1979) and is caused by *SLC4A4* defects that impair bicarbonate absorption (Igarashi et al. 1999), but the enamel is hypoplastic, as *Slc4a4* is

expressed early, during the secretory stage (Jalali et al. 2014). Hypomaturation enamel has been associated with distal renal tubular acidosis of unknown cause (Ravi et al. 2013; Misgar et al. 2017), and the enamel phenotype is similar to that caused by biallelic *WDR72* defects.

In this study, we recruited 1 African and 5 Turkish families presenting with hypomaturation autosomal recessive AI and identified 6 disease-causing *WDR72* mutations (Appendix Table 1). Only 1 of the mutations (a frameshift) had previously been reported. The novel mutations included 3 stop-gains, a missense mutation, and a 62,138–base pair deletion. Three affected members of the 6 families showed decreased serum pH (Appendix Table 2).

Materials and Methods

Enrollment of Human Subjects

The study was reviewed and approved by the Institutional Review Boards at the University of Istanbul, Seoul National University Dental Hospital, University of Pittsburgh, and University of Michigan. Five unrelated Turkish families presenting nonsyndromic hypomaturation AI were characterized and recruited by Dr. Seymen and her team. One family from the Dental Registry and DNA Repository at the University of Pittsburgh School of Dental Medicine was submitted by Dr. Jacquemont. In compliance with the Declaration of Helsinki, subject enrollment, clinical examinations, and collection of saliva samples were performed with the understanding and written consent of each participant. Medical tests were performed by the Central Biochemistry Emergency Laboratory, Istanbul Faculty of Medicine, Istanbul University.

Whole Exome Sequencing and Bioinformatics Analysis

Saliva samples were collected per standard procedures (Norgen Biotech) under the supervision of a pediatric dentist or a physician (family 3). Upon arrival, saliva samples were coded, and 300-μL aliquots were used for genomic DNA isolation following the manufacturer's protocol (Saliva-DNA-Isolation-Kit-PIRU45400-4-M14.pdf; Norgen Biotech). Genomic DNA quality was evaluated by electrophoresis on a 1.5% agarose gel and quantified with a Qubit Fluorometer (ThermoFisher Scientific). DNA samples from the probands and selected family members were characterized by whole exome sequencing at

the Johns Hopkins Center for Inherited Disease Research (CIDR). Each 50-μL sample (50-ng/μL concentration) was plated on a 96-well plate. The samples and a manifest file with coded sample information were shipped to the CIDR overnight on dry ice. Samples were genotyped with an Illumina QC Array to confirm sex and family relation before being subjected to exome capture with the Agilent SureSelect Human All Exon Enrichment System, followed by paired-end sequencing (Illumina HiSeq 2500; CIDR). Sequencing reads were aligned to human reference genome hg19 with the Burrows-Wheeler Aligner, and raw data (BAM files) were downloaded through Aspera File transfer. Secondary data analysis was then conducted by applying an established analyses pipeline containing a series of bioinformatics tools, including Samtools, Genome Analysis Tool Kit, Annovar, and VarSeq (Golden Helix). The sequence variants were annotated with dbSNP build 138 (Hintzsche et al. 2016) and filtered with a cutoff value of 0.01 for the minor allele frequency. Following the comparisons between the affected proband and unaffected family members, a list of prioritized variants was then subjected to segregation analysis. Following the genetic analysis, affected individuals from all families were contacted. Peripheral blood and urine samples from available affected individuals were collected for a basic metabolic panel, complete blood count, and routine urinalysis.

Figure 2. Family 2. (**A**) Pedigree of family 2. The proband (IV:2) is the only affected member and is indicated by an arrow. The asterisks (*) mark the 4 family members recruited for this study. The double line connecting the mother (III:7) and father (III:8) of the proband indicates consanguinity. (**B**) Clinical photo of the proband's secondary dentition at age 10 y, showing hypomaturation amelogenesis imperfecta. The sizes and shapes of the crowns appeared to be normal at the time of eruption but stained brown. (**C**) The proband's panoramic radiograph showed only minor contrast between the enamel and dentin layers. (**D**) DNA sequence chromatograms confirmed that the proband was homozygous for the *WDR72* c.1265G>T/p.(Gly422Val) missense mutation in exon 11 (left). The proband's younger brother (IV:1) showed the *WDR72* wild-type sequence at this position (right), while the mother (III:7) and father (III:8) were both heterozygous for it.

Polymerase Chain Reaction and Sanger Sequencing

The segregation of *WDR72* sequence variations within each family was determined by polymerase chain reaction (PCR) analyses carried out with the high-fidelity PCR Master Mix (ThermoFisher Scientific). The amplification products were purified (QIAquick PCR Purification Kit; Qiagen) and characterized by Sanger sequencing at the DNA Sequencing Core, University of Michigan. PCR primer sets were designed to bracket each candidate variant, and the PCRs were conducted as described in Appendix Table 3.

Results

Biallelic *WDR72* sequence variations were identified by whole exome sequencing in the recruited affected members of 6 families exhibiting autosomal recessive generalized hypomaturation AI with 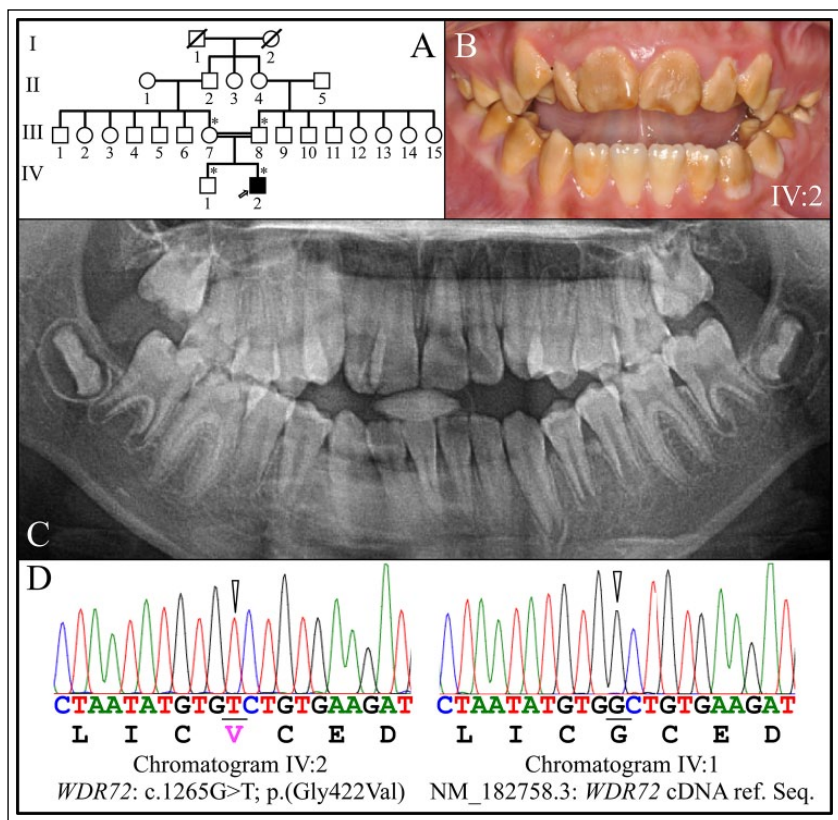accelerated dental attrition and orange-brown staining of all teeth. The *WDR72* sequence variations were confirmed, and their distributions among the recruited family members were determined by Sanger sequencing. One of the *WDR72* defects was a frameshift that was previously reported, p.(Val491Aspfs*8) (Lee et al. 2010; Wright et al. 2011), while the 5 other *WDR72* defects were novel. Three of the novel mutations were stop-gains: p.(Trp126*), p.(Arg601*), and p.(Arg784*). One was a missense mutation, p.(Gly422Val), and 1 was a 62,138–base pair deletion, g.35441_97578del62138, that included coding exons 3 through 13. These findings raise the number of reported novel disease-causing *WDR72* defects to 17 (Appendix Fig. 1; El-Sayed et al. 2009; Lee et al. 2010; El-Sayed et al. 2011; Wright et al. 2011; Kuechler et al. 2012; Katsura et al. 2014; Hentschel et al. 2016; Prasad et al. 2016).

Family 1

The proband was an 8-y-old daughter (IV:I) from a consanguineous family (Fig. 1A) who presented with generalized hypomaturation AI in the primary and secondary dentitions
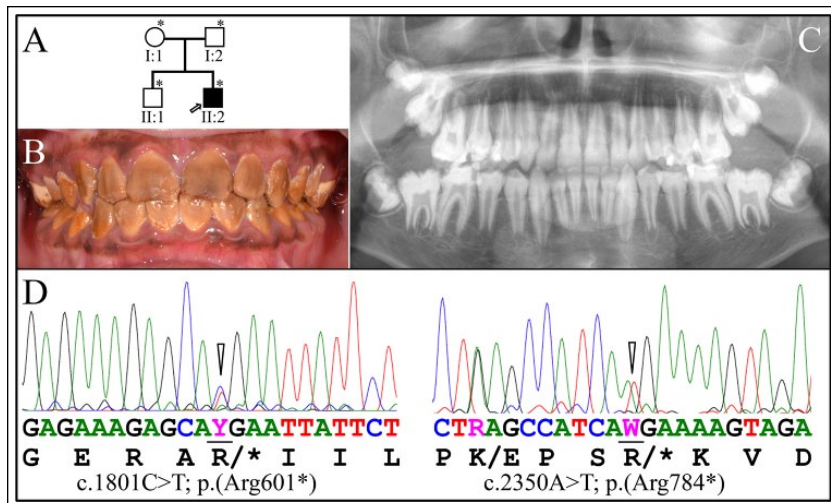
Figure 3. Family 3. (**A**) Pedigree of family 3. The proband (II:2) is the only affected member and is indicated by an arrow. Asterisks (*) mark the 4 family members recruited for this study. (**B**) Clinical photo of the proband's secondary dentition at age 12 y 7 mo, showing hypomaturation amelogenesis imperfecta. The sizes and shapes of the crowns appeared to be normal, but all of the dental crowns were deeply stained brown. (**C**) The proband's panoramic radiograph showed only minor contrast between the enamel and dentin layers and only in some places. (**D**) The proband and his father (I:2) are both heterozygous for the *WDR72* c.1801C>T/p.(Arg601*) mutation (left; Y = C or T), while the proband and his mother (I:1) are both heterozygous for the *WDR72* c.2350A>T/p.(Arg784*) stop-gain mutation (right). In this defective *WDR72* allele, there was also a nearby polymorphism (*WDR72* c.2341A>G/p.(Lys781Glu)), which is relatively common and not likely to affect function. The proband is the only person in the family who is a compound heterozygote for the 2 *WDR72* stop-gain mutations. His younger brother (II:1) has 2 normal *WDR72* alleles.

(Fig. 1B). The proband's teeth were stained brown and underwent rapid attrition. The proband also exhibited a class 3 malocclusion with crossbite. The enamel appeared brown and soft and was virtually undetectable on the panoramic radiograph (Fig. 1C). The enamel was not hypoplastic, as the sizes and shapes of erupting crowns appeared to be normal and no increased spacing of the primary teeth was observed. The AI in the proband was associated with a homozygous *WDR72* truncation mutation in exon 5: g.49333G>A, c.377G>A, p.(Trp126*) (Fig. 1D). The proband's mother (III:4), father (III:3), and sister (IV:2) were heterozygous for this *WDR72* defect [p.(Trp126*)] and showed no AI phenotype. The wild-type WDR72 protein contains 1,102 amino acids encoded by exon 2 through exon 20 (Appendix Fig. 1). It is likely that termination of translation in exon 5 would stimulate the nonsense-mediated decay (NMD) system to degrade the defective mRNA. The phenotype in the affected proband (IV:1) is unlikely to be caused by a truncated version of the WDR72 protein but rather from the complete absence of the protein (Raimondeau et al. 2018). We noted that a 50% loss of normal WDR72 (haploinsufficiency) protein in the heterozygous carriers of the WDR72 mutation is still sufficient for normal dental development.

Family 2

The proband was a 10-y-old male (IV:2) from a consanguineous family (Fig. 2A) presenting with generalized hypomaturation AI (Fig. 2B). The proband presented with an anterior open

bite and negative overjet, and his enamel was soft and brown on all teeth, although the mandibular central incisors were less stained than the rest of the dentition (Fig. 2B). The sizes and shapes of the crowns appeared to be normal at the time of eruption, with tight interdental contacts. The panoramic radiograph showed some contrast between the dentin and enamel (especially in the posterior teeth), but the enamel contrast was not as dense as normal enamel, correlating with observed enamel softness (Fig. 2C). The AI in the proband was associated with a homozygous *WDR72* p.(Gly422Val) missense mutation in exon 11 (Fig. 2D). The proband's mother (III:7) and father (III:8) were heterozygous for the *WDR72* p.(Gly422Val) mutation. The proband's sister (IV:1) did not carry the p.(Gly422Val) missense mutation on either *WDR72* allele (Fig. 2D). This sequence variation (rs367586778) is rare (0.00008 in the Grand Opportunity Exome Sequencing Project), is not listed in dbSNP, and is predicted to interfere with protein function per Sorting Intolerant from Tolerant (score = 0; Sim et al. 2012) and Polymorphism Phenotyping v2 (score = 0.999; Adzhubei et al. 2013). In this case, the altered WDR72 protein would likely be expressed but not fully functional. The proband (IV:2) was tested at age 15 y and found to have low serum pH (Appendix Table 2).

Family 3

The proband was an African male (II:2) aged 12 y 7 mo from a nonconsanguineous family presenting with generalized hypomaturation AI (Fig. 3A). The enamel was stained dark brown (Fig. 3B) and slightly contrasted with dentin on the panoramic radiograph (Fig. 3C), indicating that the enamel layer was less mineralized than normal. Two different *WDR72* stop-gain mutations were identified in this family (Fig. 3D). The proband and his father (I:2) were heterozygous for a *WDR72* c.1801C>T/p.(Arg601*) mutation (rs761647336) in exon 14, which has an allele frequency of 0.000008 in the Exome Aggregation Consortium database ("EXaC Project Pins Down Rare Gene Variants" 2016) and causes a loss of function, probably through NMD of the mutant mRNA. The proband and his mother (I:1) were both heterozygous for a *WDR72* c.2350A>T/p.(Arg784*) mutation (rs1334406422) in exon 15, which also causes a loss of function, likely through NMD of the mutant mRNA. In this defective *WDR72* allele, there was also a nearby *WDR72* c.2341A>G/p.(Lys781Glu) missense mutation, which is listed in the dbSNP database (rs60404950) with a minor allele frequency of 0.133 and is predicted to be benign with a Sorting Intolerant from Tolerant score of 0.121

and a Polymorphism Phenotyping v2 score of 0.003. The proband is the only person in the family who is a compound heterozygote for the 2 *WDR72* stop-gain mutations. His older brother (II:1) has 2 normal *WDR72* alleles. Family 3 did not undergo medical testing for kidney conditions.

Whole exome sequencing also identified a heterozygous *COL11A1* splice junction mutation (NM_080629.2:c.933+2T>C) in the mother (I:1) and proband (II:2) of family 3. In addition to the AI phenotype, the proband had joint laxity, hyperelastic skin, and recurrent nosebleeds but no history of kidney problems, middle ear infections, or other systemic conditions. *COL11A1* mutations are associated with type II Stickler syndrome (OMIM #604841; Higuchi et al. 2017) and with Marshall syndrome (OMIM #154780; Caliskan et al. 2015). Neither of these autosomal dominant conditions is associated with enamel malformations.

Family 4

The proband (IV: 6) of family 4 was a 13-y-old male presenting with generalized hypomaturation AI, dark brown staining throughout, and rapid attrition of the enamel layer (Fig. 4A). He was 1 of 4 affected individuals from a large consanguineous family (Fig. 4B), from which 10 members were recruited. On the panoramic radiograph, the enamel layer appeared to be thin with minimal contrast with dentin (Fig. 4C). The whole exome sequencing results from the proband showed no *WDR72* coverage for exons 3 through 13, indicative of a large deletion in that region (Fig. 4D). DNA sequence chromatogram of a PCR amplification product spanning the deletion precisely characterized the deletion: *WDR72* g.35441_ 97578del62138. Even if the abbreviated *WDR72* gene was expressed normally, spliced across the deletion to unite exon 2 to exon 14, and translated, the reading frame would shift [p.(Ile52Alafs*25)] after Lys51 and be followed by 24 extraneous amino acids: ALWKDMRQEKEHELFLIVV MIHSL*. The more likely consequence of the deletion, however, would be degradation of the abbreviated transcript by NMD. All 3 affected recruited members of family 4 (V:4, V:6, V:8) were homozygous for this deletion. The proband's parents were both unaffected and heterozygous for the *WDR72* deletion.
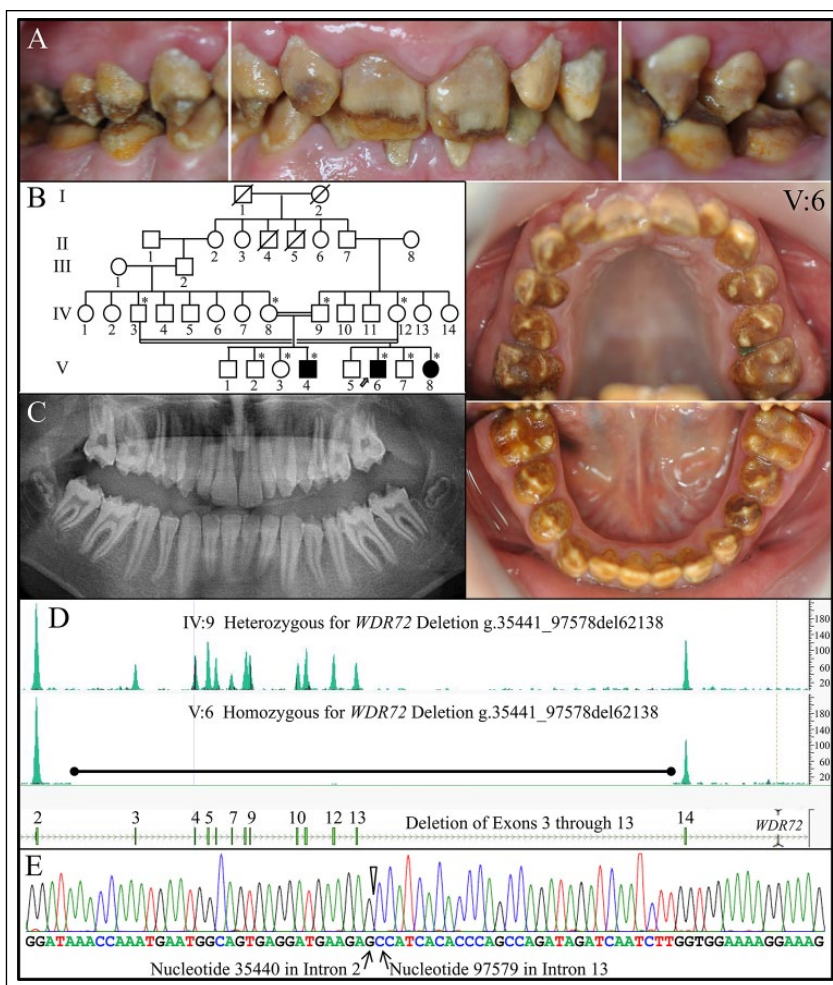

Figure 4. Family 4. (**A**) Clinical photos of the proband (V:6) at age 13 y showing generalized heavy brown staining and hypomaturation amelogenesis imperfecta in the secondary dentition. (**B**) Pedigree of family 4. Asterisks (*) mark the 9 family members recruited for this study. The proband is indicated with an arrow. The double lines connecting the father (IV:3) and mother (IV:12) of the proband and his aunt (IV:8) and uncle (IV:9) indicate consanguinity. (**C**) The proband's panoramic radiograph taken at age 13 y shows very little enamel contrasting with dentin. (**D**) Whole exome sequencing results showed no coverage for *WDR72* for exons 3 through 13 in the proband (top). DNA sequence chromatogram of a polymerase chain reaction amplification product spanning the deletion demonstrated that the *WDR72* deletion was g.35441_97578del62138 (bottom). All 3 affected recruited members of family 4 (V:4, V:6, V:8) were homozygous for this deletion.

Family 5

Although family 5 had no known connection to family 4, genetic analysis demonstrated that the proband had the same 62,138–base pair deletion in *WDR72* that affected family 4. The proband (IV:4) was the only affected member of family 5 (Appendix Fig. 2). Her primary dentition was stained brown and exhibited severe dental attrition, which caused dental abscesses in the maxillary central incisors. Generalized hypomaturation enamel often fractures following eruption of the defective teeth into occlusion and does not contrast with dentin radiographically (Appendix Fig. 2C). The distribution of
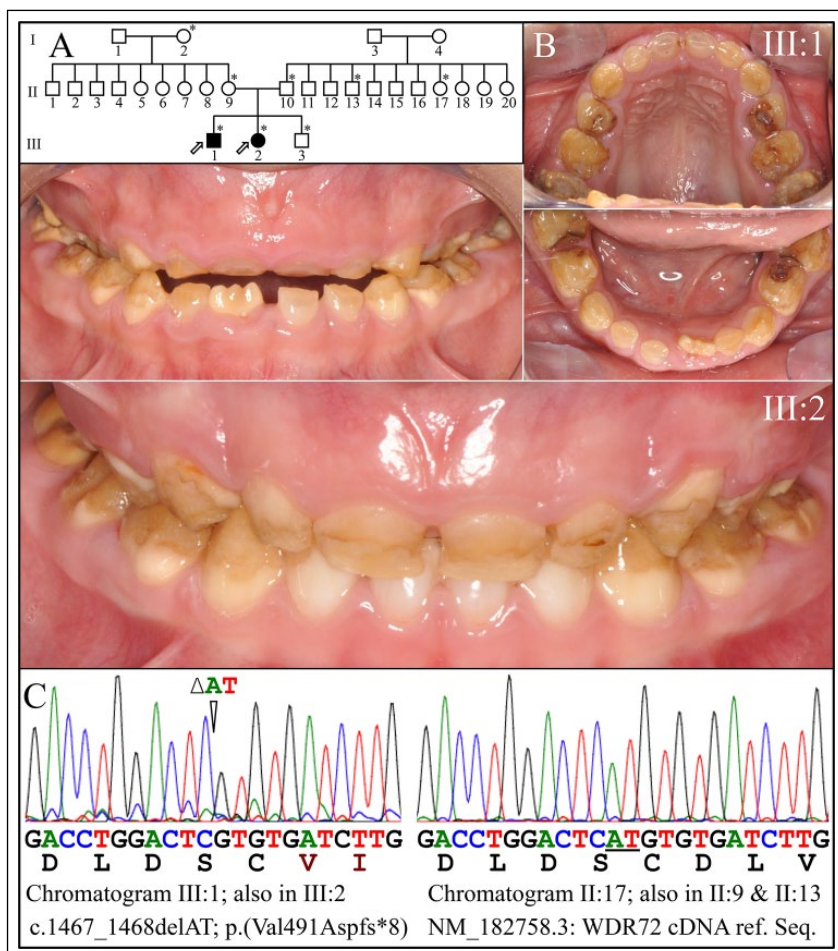
Discussion

Dental enamel is a highly organized acellular mineral that is deposited on mineralized dentin by a sheet of epithelial cells called *ameloblasts* (Simmer and Fincham 1995). Enamel forms in stages. Proteins are secreted by secretory-stage ameloblasts into a defined extracellular space that expands as enamel ribbons lengthen (Simmer et al. 2010; Simmer et al. 2012). Once the enamel layer achieves its final thickness, the enamel-forming cells transition into maturation-stage ameloblasts that modulate between ruffled- and smooth-ended phases to harden the enamel layer, principally by transporting ions and actively removing water and residual organic matrix (Smith 1998; Lacruz et al. 2013). Clinically, the observation of a hypomineralized enamel layer (which does not contrast with dentin on radiographs) of normal thickness suggests that a disturbance occurred during the maturation stage, which is characteristic of the AI cases caused by the *WDR72* defects reported here.

There is increasing evidence that *WDR72* defects cause syndromic, rather than isolated, AI. *Wdr72* is intact in 4 edentulous taxa and 3 taxa with enamelless teeth, demonstrating evolutionary selection pressure for *Wdr72* beyond its involvement in tooth development (Springer et al. 2016). A genome-wide study associated *WDR72* mutations with neurocognitive function (LeBlanc et al. 2012), although none of the papers reporting the 17 recessive AI-causing *WDR72* defects observed neurocognitive deficits. Hypomaturation AI and mild short stature were observed in 2 individuals with homozygous *WDR72* mutations (Kuechler et al. 2012). Height and weight measurements of 8 individuals with AI caused by biallelic *WDR72* defects in this study did not show a consistent pattern of short stature. As many individuals were above the 50th percentile for height and weight as were below it (Appendix Table 2). A series of studies determined that *WDR72* is necessary for proper kidney function. *WDR72* was among 7 loci suspected to affect creatinine production and secretion by the kidneys (Kottgen et al. 2010). Decreased estimated glomerular filtration rate and albuminuria were associated with single-nucleotide polymorphisms in *WDR72* in American Indians (Franceschini et al. 2014). Most recently, *WDR72* mutations were shown to cause distal renal tubular acidosis (Rungroj et al. 2018), where the kidneys do not adequately transfer acids from blood to urine, causing acidosis.

Figure 5. Family 6. (**A**) Pedigree of family 6. Seven asterisks (*) identify family members recruited for this study. (**B**) Clinical photos of the first proband (III:1) at age 6 y show generalized hypomaturation amelogenesis imperfecta. (**C**) Clinical photos of the second proband (III:2) at age 5 y. (**D**) Chromatogram of proband III:1 that identifies a homozygous AT deletion (c._1467_1468/p.Val491Aspfs*8) in *WDR72* (left). The resulting frameshift would add DLVGYLY* after Cys490. The father (II:10), grandmother (II:9), and unaffected sibling (III:3) were heterozygous for AT deletion and had normal enamel (not shown).

WDR72 g.35441_97578del62138 deletion in family 4 and family 5 was determined by PCR analyses (Appendix Fig. 3).

Family 6

The probands, a 6-year-old male and a 5-year-old female, were the only members of this large family who were affected with AI (Fig. 5). Eight members of the family were recruited. Both probands presented with generalized hypomaturation AI with rapid attrition (Fig. 5B). The teeth stained brown, particularly in places where the enamel had fractured away (Fig. 5B). The 2 probands were homozygous for a *WDR72* exon 12 frameshift mutation [c.1467_1468/p.(Val491Aspfs*8)] that was previously reported to cause autosomal recessive hypomaturation AI (Lee et al. 2010; Wright et al. 2011). The probands, III:1 and III:2, were tested at ages 11 and 10 y, respectively, and found to have low serum pH (Appendix Table 2).

Our finding of low serum pH in 3 of 8 affected persons tested supports these findings. Three of 8 affected persons also had low serum creatinine, which may be associated with muscle loss, liver disease, or protein deficiency (Appendix Table 2).

As more is learned about the genetic etiologies of inherited enamel defects, it is increasingly clear that isolated and syndromic forms of AI cannot be distinguished clinically on the basis of the dental phenotype. Kidney and dental enamel problems are now associated with biallelic defects in *FAM20A* (Jaureguiberry et al. 2012; Wang et al. 2013), *CLDN16* (Bardet et al. 2016), *CLDN19* (Yamaguti et al. 2017), *SLC4A4* (Igarashi et al. 1999), and *WDR72* (Rungroj et al. 2018). With advances in our understanding of the genetic etiologies of inherited enamel malformations, genetic testing is increasingly able to determine the cause of AI in a given family and enable interventions to manage AI-associated systemic conditions.

Author Contributions

H. Zhang, contributed to data analysis and interpretation, critically revised the manuscript; M. Koruyucu, contributed to data acquisition and interpretation, critically revised the manuscript; F. Seymen, contributed to data acquisition, analysis, and interpretation, critically revised the manuscript; Y. Kasimoglu, contributed to data acquisition and interpretation, critically revised the manuscript; J.W. Kim, contributed to design, data analysis and interpretation, critically revised the manuscript; S. Tinawi, contributed to data interpretation, drafted and critically revised the manuscript; C. Zhang, contributed to analysis, critically revised the manuscript; M.L. Jacquemont, A.R. Vieira, contributed to data acquisition, critically revised the manuscript; J.P. Simmer, contributed to conception, design, data analysis and interpretation, drafted and critically revised the manuscript; J.C.C. Hu, contributed to conception and design, data acquisition, analysis, and interpretation, drafted and critically revised the manuscript. All authors gave final approval and agree to be accountable for all aspects of the work.

Acknowledgments

ORCID iDs

J.W. Kim https://orcid.org/0000-0002-9399-2197
A.R. Vieira https://orcid.org/0000-0003-3392-6881

References

Adzhubei I, Jordan DM, Sunyaev SR. 2013. Predicting functional effect of human missense mutations using polyphen-2. Curr Protoc Hum Genet. Chap 7, unit 7.20.

Bardet C, Courson F, Wu Y, Khaddam M, Salmon B, Ribes S, Thumfart J, Yamaguti PM, Rochefort GY, Figueres ML, et al. 2016. Claudin-16 deficiency impairs tight junction function in ameloblasts, leading to abnormal enamel formation. J Bone Miner Res. 31(3):498–513.

Burgueno Torres L, Mourelle Martinez MR, de Nova Garcia JM. 2015. A study on the chronology and sequence of eruption of primary teeth in Spanish children. Eur J Paediatr Dent. 16(4):301–304.

Caliskan E, Acikgoz G, Yeniay Y, Ozmen I, Gamsizkan M, Akar A. 2015. A case of Marshall's syndrome and review of the literature. Int J Dermatol. 54(6):e217–e221.

El-Sayed W, Parry DA, Shore RC, Ahmed M, Jafri H, Rashid Y, Al-Bahlani S, Al Harasi S, Kirkham J, Inglehearn CF, et al. 2009. Mutations in the beta propeller WDR72 cause autosomal-recessive hypomaturation amelogenesis imperfecta. Am J Hum Genet. 85(5):699–705.

El-Sayed W, Shore RC, Parry DA, Inglehearn CF, Mighell AJ. 2011. Hypomaturation amelogenesis imperfecta due to WDR72 mutations: a novel mutation and ultrastructural analyses of deciduous teeth. Cells Tissues Organs. 194(1):60–66.

EXaC project pins down rare gene variants. 2016. Nature. 536(7616):249.

Franceschini N, Haack K, Almasy L, Laston S, Lee ET, Best LG, Fabsitz RR, MacCluer JW, Howard BV, Umans JG, et al. 2014. Generalization of associations of kidney-related genetic loci to American Indians. Clin J Am Soc Nephrol. 9(1):150–158.

Hentschel J, Tatun D, Parkhomchuk D, Kurth I, Schimmel B, Heinrich-Weltzien R, Bertzbach S, Peters H, Beetz C. 2016. Identification of the first multi-exonic WDR72 deletion in isolated amelogenesis imperfecta, and generation of a WDR72-specific copy number screening tool. Gene. 590(1):1–4.

Higuchi Y, Hasegawa K, Yamashita M, Tanaka H, Tsukahara H. 2017. A novel mutation in the COL2A1 gene in a patient with stickler syndrome type 1: a case report and review of the literature. J Med Case Rep. 11(1):237.

Hintzsche J, Kim J, Yadav V, Amato C, Robinson SE, Seelenfreund E, Shellman Y, Wisell J, Applegate A, McCarter M, et al. 2016. Impact: a whole-exome sequencing analysis pipeline for integrating molecular profiles with actionable therapeutics in clinical samples. J Am Med Inform Assoc. 23(4):721–730.

Igarashi T, Inatomi J, Sekine T, Cha SH, Kanai Y, Kunimi M, Tsukamoto K, Satoh H, Shimadzu M, Tozawa F, et al. 1999. Mutations in SLC4A4 cause permanent isolated proximal renal tubular acidosis with ocular abnormalities. Nat Genet. 23(3):264–266.

Jalali R, Guo J, Zandieh-Doulabi B, Bervoets TJ, Paine ML, Boron WF, Parker MD, Bijvelds MJ, Medina JF, DenBesten PK, et al. 2014. NBCe1 (SLC4A4) a potential pH regulator in enamel organ cells during enamel development in the mouse. Cell Tissue Res. 358(2):433–442.

Jaureguiberry G, De la Dure-Molla M, Parry D, Quentric M, Himmerkus N, Koike T, Poulter J, Klootwijk E, Robinette SL, Howie AJ, et al. 2012. Nephrocalcinosis (enamel renal syndrome) caused by autosomal recessive FAM20A mutations. Nephron Physiol. 122(1–2):1–6.

Katsura KA, Horst JA, Chandra D, Le TQ, Nakano Y, Zhang Y, Horst OV, Zhu L, Le MH, DenBesten PK. 2014. WDR72 models of structure and function: a stage-specific regulator of enamel mineralization. Matrix Biol. 38:48–58.

Kottgen A, Pattaro C, Boger CA, Fuchsberger C, Olden M, Glazer NL, Parsa A, Gao X, Yang Q, Smith AV, et al. 2010. New loci associated with kidney function and chronic kidney disease. Nat Genet. 42(5):376–384.

Kuechler A, Hentschel J, Kurth I, Stephan B, Prott EC, Schweiger B, Schuster A, Wieczorek D, Ludecke HJ. 2012. A novel homozygous WDR72 mutation in two siblings with amelogenesis imperfecta and mild short stature. Mol Syndromol. 3(5):223–229.

Lacruz RS, Smith CE, Kurtz I, Hubbard MJ, Paine ML. 2013. New paradigms on the transport functions of maturation-stage ameloblasts. J Dent Res. 92(2):122–129.

LeBlanc M, Kulle B, Sundet K, Agartz I, Melle I, Djurovic S, Frigessi A, Andreassen OA. 2012. Genome-wide study identifies PTPRO and WDR72 and FOXQ1-SUMO1P1 interaction associated with neurocognitive function. J Psychiatr Res. 46(2):271–278.

Lee SK, Seymen F, Lee KE, Kang HY, Yildirim M, Tuna EB, Gencay K, Hwang YH, Nam KH, De La Garza RJ, et al. 2010. Novel WDR72 mutation and cytoplasmic localization. J Dent Res. 89(12):1378–1382.

Misgar RA, Hassan Z, Wani AI, Bashir MI. 2017. Amelogenesis imperfecta with distal renal tubular acidosis: a novel syndrome? Indian J Nephrol. 27(3):225–227.

Prasad MK, Geoffroy V, Vicaire S, Jost B, Dumas M, Le Gras S, Switala M, Gasse B, Laugel-Haushalter V, Paschaki M, et al. 2016. A targeted next-generation sequencing assay for the molecular diagnosis of genetic disorders with orodental involvement. J Med Genet. 53(2):98–110.

Raimondeau E, Bufton JC, Schaffitzel C. 2018. New insights into the interplay between the translation machinery and nonsense-mediated mRNA decay factors. Biochem Soc Trans. 46(3):503–512.

Ravi P, Ekambaranath TS, Arasi SE, Fernando E. 2013. Distal renal tubular acidosis and amelogenesis imperfecta: a rare association. Indian J Nephrol. 23(6):452–455.

Rungroj N, Nettuwakul C, Sawasdee N, Sangnual S, Deejai N, Misgar RA, Pasena A, Khositseth S, Kirdpon S, Sritippayawan S, et al. 2018. Distal renal tubular acidosis caused by tryptophan-aspartate repeat domain 72 (WDR72) mutations. Clin Genet. 94(5):409–418.

Sim NL, Kumar P, Hu J, Henikoff S, Schneider G, Ng PC. 2012. SIFT web server: predicting effects of amino acid substitutions on proteins. Nucleic Acids Res. 40(Web Server issue):W452–W457.

Simmer JP, Fincham AG. 1995. Molecular mechanisms of dental enamel formation. Crit Rev Oral Biol Med. 6(2):84–108.

Simmer JP, Papagerakis P, Smith CE, Fisher DC, Rountrey AN, Zheng L, Hu JC. 2010. Regulation of dental enamel shape and hardness. J Dent Res. 89(10):1024–1038.

Simmer JP, Richardson AS, Hu YY, Smith CE, Hu JC-C. 2012. A post-classical theory of enamel biomineralization . . . and why we need one. Int J Oral Sci. 4(3):129–134.

Simmer JP, Richardson AS, Wang SK, Reid BM, Bai Y, Hu Y, Hu JC. 2014. Ameloblast transcriptome changes from secretory to maturation stages. Connect Tissue Res. 55 Suppl 1:29–32.

Smith CE. 1998. Cellular and chemical events during enamel maturation. Crit Rev Oral Biol Med. 9(2):128–161.

Smith CEL, Poulter JA, Antanaviciute A, Kirkham J, Brookes SJ, Inglehearn CF, Mighell AJ. 2017. Amelogenesis imperfecta: genes, proteins, and pathways. Front Physiol. 8:435.

Springer MS, Starrett J, Morin PA, Lanzetti A, Hayashi C, Gatesy J. 2016. Inactivation of C4orf26 in toothless placental mammals. Mol Phylogenet Evol. 95:34–45.

Stirnimann CU, Petsalaki E, Russell RB, Muller CW. 2010. WD40 proteins propel cellular networks. Trends Biochem Sci. 35(10):565–574.

Wang SK, Aref P, Hu Y, Milkovich RN, Simmer JP, El-Khateeb M, Daggag H, Baqain ZH, Hu JC. 2013. FAM20A mutations can cause enamel-renal syndrome (ERS). PLoS Genet. 9(2):e1003302.

Wang SK, Hu Y, Yang J, Smith CE, Nunez SM, Richardson AS, Pal S, Samann AC, Hu JC, Simmer JP. 2015. Critical roles for WDR72 in calcium transport and matrix protein removal during enamel maturation. Mol Genet Genomic Med. 3(4):302–319.

Winsnes A, Monn E, Stokke O, Feyling T. 1979. Congenital persistent proximal type renal tubular acidosis in two brothers. Acta Paediatr Scand. 68(6):861–868.

Wright JT, Carrion IA, Morris C. 2015. The molecular basis of hereditary enamel defects in humans. J Dent Res. 94(1):52–61.

Wright JT, Torain M, Long K, Seow K, Crawford P, Aldred MJ, Hart PS, Hart TC. 2011. Amelogenesis imperfecta: genotype-phenotype studies in 71 families. Cells Tissues Organs. 194(2–4):279–283.

Xu C, Min J. 2011. Structure and function of WD40 domain proteins. Protein Cell. 2(3):202–214.

Yamaguti PM, Neves FA, Hotton D, Bardet C, de La Dure-Molla M, Castro LC, Scher MD, Barbosa ME, Ditsch C, Fricain JC, et al. 2017. Amelogenesis imperfecta in familial hypomagnesaemia and hypercalciuria with nephrocalcinosis caused by CLDN19 gene mutations. J Med Genet. 54(1):26–37.